Verification of the Generalized Scaling Law for Flat Layered Sand Deposit

T. Tobita[1], S. Escoffier[2], J. L. Chazelas[2] and S. Iai[1]
[1] *Disaster Prevention Research Institute, Kyoto University, Japan*
[2] *IFSTTAR, Nantes, France*
E-mail: tobita.tetsuo.8e@kyoto-u.ac.jp

ABSTRACT: To verify the generalized scaling law, dynamic centrifuge tests under two different centrifugal accelerations of 25 g and 50 g are conducted. The model ground constitutes of a flat dry sand layer. With the scaling law, a prototype ground is scaled down to 1/100. A sinusoidal input acceleration of frequency 1.0 Hz, maximum amplitude 0.5 g, and duration 14 sec in prototype scale is applied to the model ground. Each model is exposed to the identical input motion sequentially 10 times. In total nine accelerometers are installed in the model. Surface settlements are measured by laser displacement transducers. Settlements at three different depths (300, 200 and 50 mm – model scale - from the surface) are measured by settlement gauges. Response acceleration and penetrometer resistance show good agreements in prototype scale. Measured settlements after the initial shake in prototype scale also show significant agreements between the two models when the intensity of shaking is nearly identical. As shaking continues discrepancy in settlement becomes large due to minor differences of input acceleration levels and random error associated with model constructions.

1. INTRODUCTION

In the centrifuge model testing, although structural models have to be small and simplified, the prototype behaviour is approximated in accordance with scaling laws (e.g., Garnier et al., 2007), and it qualitatively represents prototype behaviour. One of the major obstacles for application of physical modelling results to performance-based design practice is that a specific prototype cannot be tested due to restrictions associated with experimental conditions, such as the size of the model container and scaling effects on materials. For 1-g model testing, to overcome these restrictions, the size of the experimental facility has become larger and larger so that real-scale models can be tested [e.g., E-defense (Tokimatsu et al., 2007), NEES@UC San Diego Large High Performance Outdoor Shake Table (Einde et al., 2004)]. However, for geotechnical structures, development of larger research facility may still have limitations because, even with such a large facility, physical modelling with foundations and surrounding ground has to be reduced due to factors inherent in a large facility, such as the capacity of the shake table and budget.

Demands for the testing of large prototypes are increasing under the restrictions mentioned above. To resolve such demands and restrictions, Iai et al. (2005) proposed a scaling law by combining the scaling law for centrifuge testing with the one for 1-g dynamic-model testing. They call it the “generalized scaling law” in dynamic centrifuge modelling. Tobita et al. (2011) investigated its applicability with a flat saturated sand bed. They conducted a series of centrifuge model tests to verify and find issues on the generalized scaling law under the scheme of the modelling of models technique. In a series of dynamic tests, four different centrifugal accelerations from 5 g to 70 g are applied to the scaled models for which the prototype is uniquely given. With the scaling law, the prototype is scaled down to 1/100. The models are exposed to sinusoidal input accelerations with 0.65 Hz and amplitudes of 2.1 m/s^2 and 3.1 m/s^2 in prototype scale. For response during shaking, nearly identical accelerations and excess pore-water pressure buildups are recorded for all the cases in the prototype scale. Discrepancies are found on surface settlements and duration time for dissipation of excess pore-water pressure. The major cause of the discrepancy of the latter “duration time” may be associated with low confining stress in model ground under low centrifugal acceleration (Haigh et al., 2012). The cause of discrepancy of surface settlement has been yet to be identified.

In this study, the applicability of the generalized scaling law, in particular, the scaling law for displacement is investigated.

1.1 Brief review of the generalized scaling law

Scaling factors for physical model tests can be introduced in general forms by choosing a set of basic physical properties to be independent and deriving the scaling factors for other properties via governing equations of the analysed system. In the concept of the generalized scaling law, a model on a shaking table in a geotechnical centrifuge is considered to be a small scale representation of a 1-g shaking-table test. Figure 1 visualizes this concept by introducing a virtual 1-g model to which the prototype is scaled down via a similitude for 1-g shaking-table tests (Iai, 1989). The virtual 1-g model is subsequently scaled down by applying a similitude for centrifuge tests to the actual physical model. In this way, the geometric scaling factors applied in 1-g tests (μ) [row (1) of Table 1] can be multiplied with those for centrifuge tests (η) [row (2) of Table 1], resulting in much larger overall scaling factors λ=μη [row (3) of Table 1].

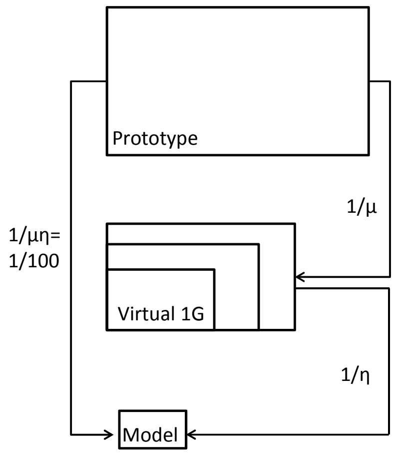

Figure 1 Relationship among prototype, virtual 1G model and centrifuge model for the case of scaling factor of 1/100 (λ=μη=100)

1.2. Issues pointed out by the past studies (Tobita et al. 2011)

To investigate the applicability of the generalized scaling law, Tobita et al. (2011) applied it to the cases of a flat saturated sand layer. In a rigid sand box filled with saturated sand (Dr=30 to 40%), accelerometers, pore water and earth pressure transducers, thermometers, and laser displacement transducers were implemented as shown in Figure 2.

Table 1 Scaling factors in physical model testing (Iai, 1989, and Iai, et al. 2005)

	(1) Scaling factors for 1g test	(2) Scaling factors for centrifuge test	(3) Generalized scaling factors
Length	μ	η	$\mu\eta$
Density	1	1	1
Time	$\mu^{0.75}$	η	$\mu^{0.75}\eta$
Frequency	$\mu^{-0.75}$	$1/\eta$	$\mu^{-0.75}/\eta$
Acceleration	1	$1/\eta$	$1/\eta$
Velocity	$\mu^{0.75}$	1	$\mu^{0.75}$
Displacement	$\mu^{1.5}$	η	$\mu^{1.5}\eta$
Stress	μ	1	μ
Strain	$\mu^{0.5}$	1	$\mu^{0.5}$
Stiffness	$\mu^{0.5}$	1	$\mu^{0.5}$
Permeability	$\mu^{0.75}$	η	$\mu^{0.75}\eta$
Pore pressure	μ	1	μ
Fluid Pressure	μ	1	μ

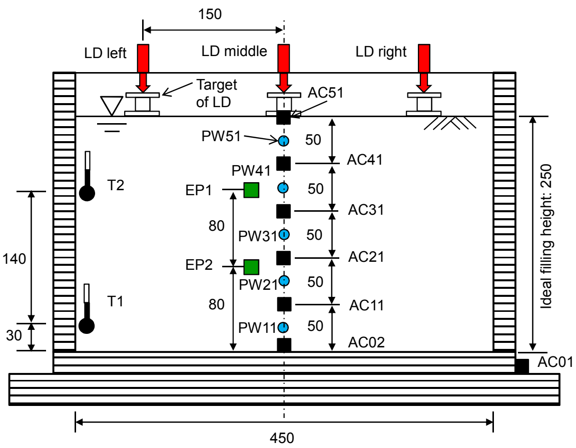

Figure 2 Test setup. LD: Laser displacement transducers. AC: Accelerometers. PW: Pore-water pressure transducers. EP: Earth pressure transducers. T: Thermometers [Tobita et al (2011)]

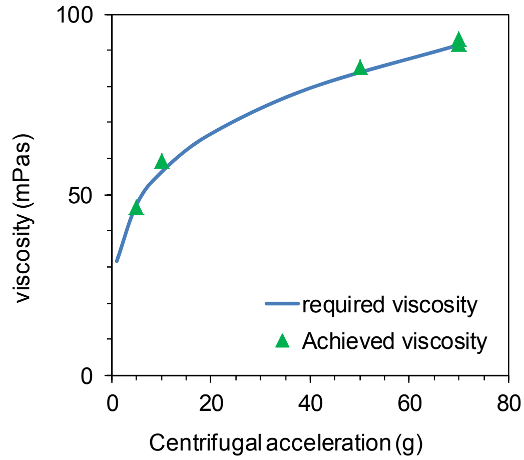

Figure 3 Achieved and required fluid viscosity [Tobita et al (2011)]

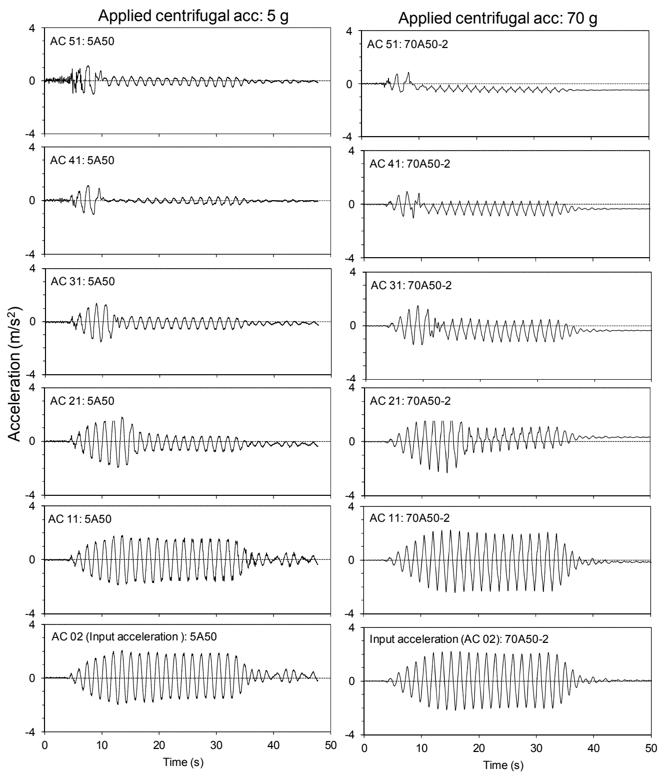

Figure 4 Measured time histories of acceleration in prototype scale: Cases 5g and 70 g [Tobita et al (2011)]

To satisfy the scaling law for the duration time of the pore water pressure dissipation, the methylcellulose solution was used for saturation of the model ground by adjusting its viscosity so that required viscosity was attained at a certain centrifugal accelerations (Figure 3). In what follows, some of the significant results and issues pointed out by Tobita et al. (2011) are presented.

Figure 4 compares acceleration response of the model ground in prototype scale. Applied centrifugal acceleration is 5 g and 70 g. Nearly identical input acceleration (AC02) was given at the base of the sand box. As shaking continues, the amplitude of acceleration in ground and at the surface are reducing due to liquefaction. In both cases, the shape and peak values of the acceleration time histories are similar, validating the applicability of the generalized scaling law for acceleration.

Time histories of excess pore water pressure build-up for the applied centrifugal acceleration of 5, 10, 50, and 70 g, are plotted in prototype scale in Figure 5. These figures also validate the applicability of the scaling for pressures.

What have not confirmed in this series of tests are the scaling low for (1) the duration time of excess pore water pressure dissipation (time for consolidation) and (2) the ground surface settlements (displacement). For (1), the duration time of dissipation took long in the case of the low centrifugal accelerations (less than 10 g). This fact may suggest the limitation of the applicability of the scaling law. It is known from the theory of 1D consolidation that small elastic stiffness leads to a long duration time for consolidation. Thus in the paper, influence of the scaling of stiffness on the time of the pore water dissipation was investigated. Another cause of this is thought to be associated with the chemical properties of viscous water. After conducting falling head permeability tests with the viscous solution, we found (Figure 6) reduction of permeability with duration time of flow, i.e., volume of fluid passing through the specimen. We suspect that long chains of polymer constituting methylcellulose ether are caught in the pores or absorbed on sand particles.

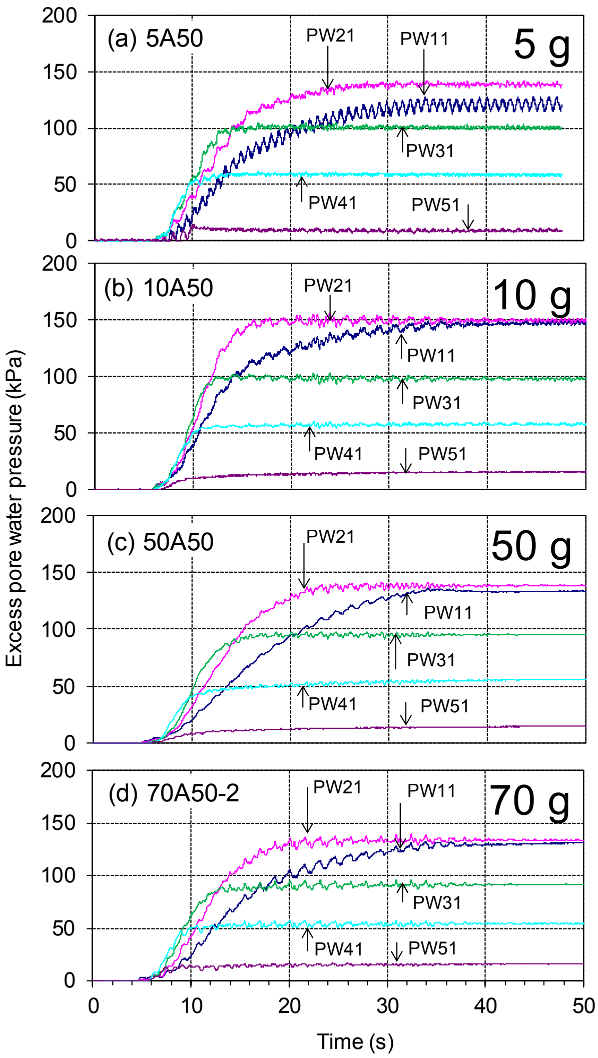

Figure 5 Measured time histories of excess pore-water pressure in the phase of pressure buildup in prototype scale (0–50 s) [Tobita et al (2011)]

For (2), issues are found that the generalized scaling law requires precise measurement of displacement because as shown in Table 1, the scaling factor of "displacement" is expressed as $\mu^{1.5}\eta$, which becomes 447 and 120 for given centrifugal accelerations of 5 g and 70 g, respectively. Compared with other physical parameters, these scaling factors of displacement are quite large. In the test shown in Figure 2, surface displacements were measured by the laser displacement transducers with targets placed on the ground surface. With this test setup, surface settlements (displacements) could not properly be measured, because the dissipating water due to liquefaction made the target position unstable. Therefore, the validity of the generalized scaling law for displacement was left out of the conclusions.

2. DYNAMIC CENTRIFUGE TESTS ON FLAT, LOOSE, DRY SAND DEPOSIT

To investigate the applicability of the generalized scaling law described above, a series of dynamic tests was conducted following the principle of "modelling of models." This technique was introduced by Schofield (1980) to assess the behaviour of a prototype through repetition of the test at different scales and comparison of the results in prototype scale. In the present study, without changing the actual size of the physical model but varying the virtual 1-g dimension, the overall scaling factor ($\lambda=\mu\eta=100$) is kept constant (Figure 1).

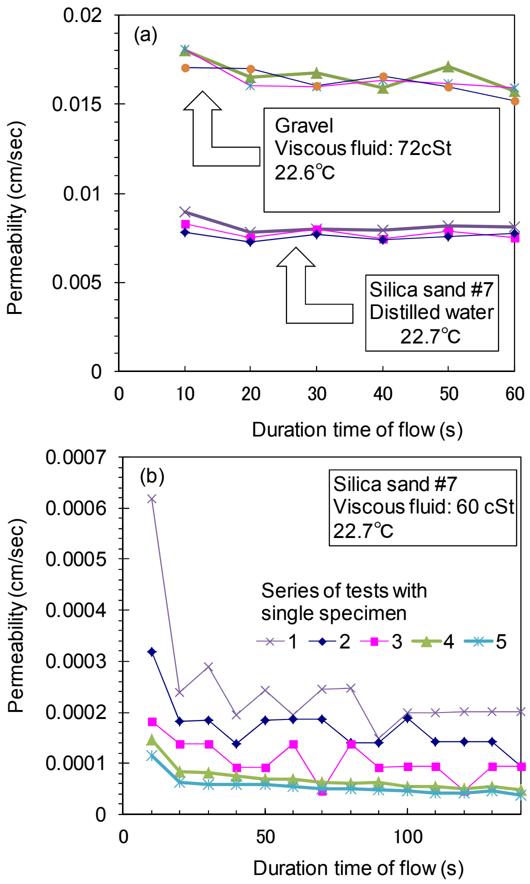

Figure 6 Variation of the permeability with duration time of flow: (a) Silica sand (Dr=40%) and distilled water, and Gravel (Dr=40%) and viscous water, (b) Silica sand (Dr=40%) and visocus water. In (b), in the series of tests, single specimen was used continuously.

Here, the overall scaling factor is set to a fixed value comprising different combinations of the scaling factors for 1-g model testing, μ, and centrifuge testing, η. Table 2 lists the applied geometric scaling factors as well as frequencies and amplitudes of the input motions employed in the study. As shown in Table 2, the scaling factors of displacement are relatively larger than the other physical quantities (200 in 25 g and 141.42 in 50g). As mentioned earlier, this fact demands precise measurements in displacement. In total 5 tests [3 tests in 25 g (25 g_1, 25g_2, and 25g_3) and 2 tests in 50 g (50g_1 and 50g_2)] are conducted. In what follows, units are in prototype unless otherwise specified.

Table 2 Test cases and scaling factors used in the present study

	Case 1	25 G		Case 2	50 G	
Quantity	scaling factor 1g test	scaling factor centrifuge test	generalized scaling factors	scaling factor 1g test	scaling factor centrifuge test	generalized scaling factors
Length	4.00	25.00	100.00	2.00	50.00	100.00
Density	1.00	1.00	1.00	1.00	1.00	1.00
Time	2.83	25.00	70.71	1.68	50.00	84.09
Frequency	0.35	0.04	0.01	0.59	0.02	0.01
Acceleration	1.00	0.04	0.04	1.00	0.02	0.02
Velocity	2.83	1.00	2.83	1.68	1.00	1.68
Displacement	8.00	25.00	200.00	2.83	50.00	141.42
Stress	4.00	1.00	4.00	2.00	1.00	2.00
Strain	2.00	1.00	2.00	1.41	1.00	1.41
Stiffness	2.00	1.00	2.00	1.41	1.00	1.41
Permeability	2.83	25.00	70.71	1.68	50.00	84.09
Pore pressure	4.00	1.00	4.00	2.00	1.00	2.00
Fluid Pressure	4.00	1.00	4.00	2.00	1.00	2.00

2.1 Test setup

A series of dynamic tests under two different centrifugal accelerations of 25 g and 50 g are conducted with the geotechnical centrifuge (arm length=5.0 m) at the IFSTTAR (Institut français des sciences et technologies des transports, de l'aménagement et des réseaux), Nantes, France. The model ground constitutes of a flat dry sand layer, which is constructed with air-pluviation method (pluviation height=0.6 m, slot width=4 mm) to form the relative density of 50% of the Fontainebleau sand NE34 (e_{min}=0.545, e_{max}=0.866). With the scaling law, a prototype ground is scaled down to 1/100. Thus, the depth of the ground in prototype scale is 41.6 m. The flexible ESB (equivalent shear beam) box whose inside dimension is 800 (W) x 416 (H) x 340 (D) (mm) in model scale is employed (Figure 7). A sinusoidal input acceleration of frequency 1.0 Hz, maximum amplitude 0.5 g, and duration 14 sec is applied to the model ground. Each model is exposed to the identical input motion sequentially 10 times in order to increase the number of measurements so that large number of comparable data can be obtained.

In total nine accelerometers are installed in the model (Figure 7). Surface settlements are measured by laser displacement transducers. Settlements at three different depths (300, 200 and 50 mm – model scale - from the surface) are measured by settlement gauges, which are made of a plate, and a rod connected to potentiometers (Figure 8, 9).

Settlement gauges are carefully placed at the specified depth (Figure 9) with fishing strings. The PVC plates without attaching the potentiometers are installed for comparison purposes. Three potentiometers are mounted after completing model ground.

3. RESPONSE OF THE MODEL GROUND

3.1 Input and ground acceleration

As shown in Figure 10, nearly identical input accelerations are given to the model ground. Figure 11 summarizes intensity of input motion in the form of Arias intensity (Eq. 1)(Arias 1970) for all the cases employed in the present study.

$$I_A = \frac{\pi}{2g}\int_0^T a(t)^2\,dt \quad \text{(m/s)} \tag{1}$$

where I_A: Arias intensity (m/s), $a(t)$: acceleration, and T: duration of shaking (16 sec in this study).

As shown in Figure 11, at all the shaking, the intensity is almost identical, except for the first 4 cases in 50 g tests. This variation may be due to the instability of shake table controller. As explained later, this variation might cause significant difference on ground settlements in the case of 50g_1.

3.2 Penetration resistance

Before the initial shaking and after the 10th shaking, the soil penetration resistance of the model ground was measured by the miniature penetrometer. As shown in Figure 12(a), the penetration resistance in depth under 50 g in model scale is, as it is expected, larger than that of 25 g. While the profiles of the resistance in prototype scale [Figure 12(b)] show that the resistance measured under 50 g is systematically smaller than the ones obtained under 25 g. Cause of this is unknown yet, and further investigation is necessary to know the limit of application of the generalized scaling law.

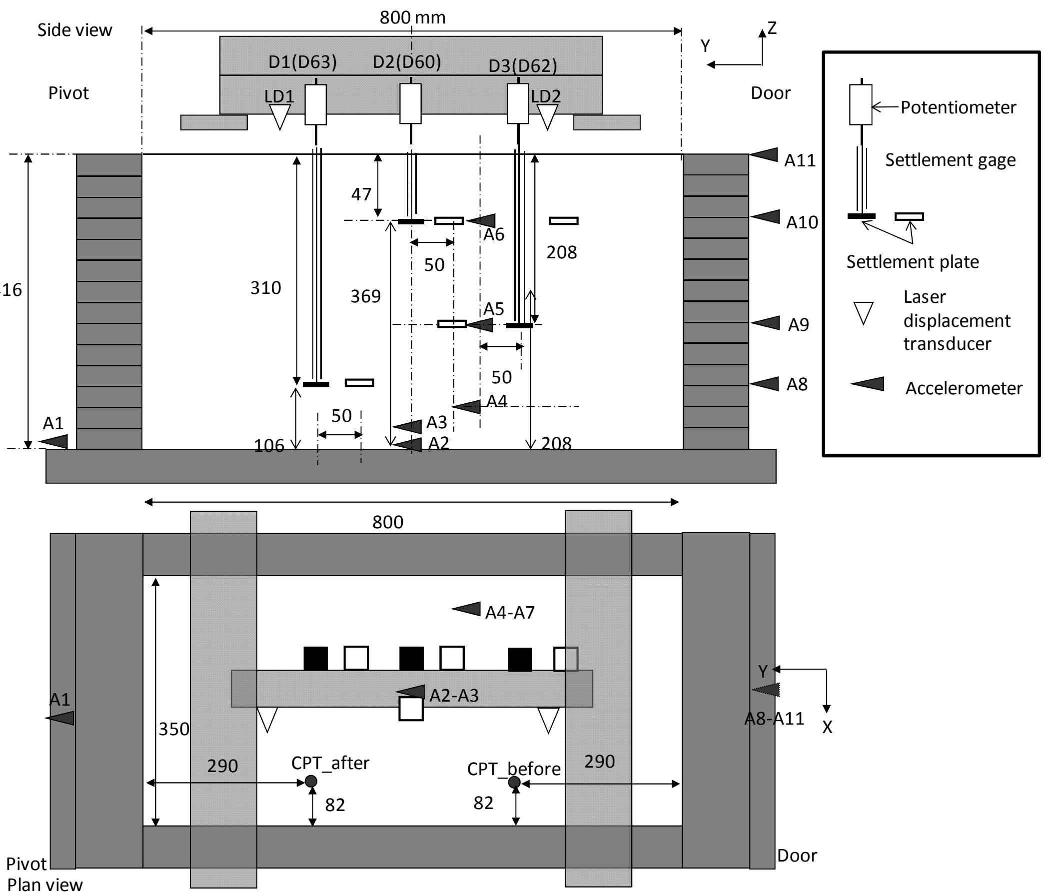

Figure 7 Schematic view and sensor location of the model

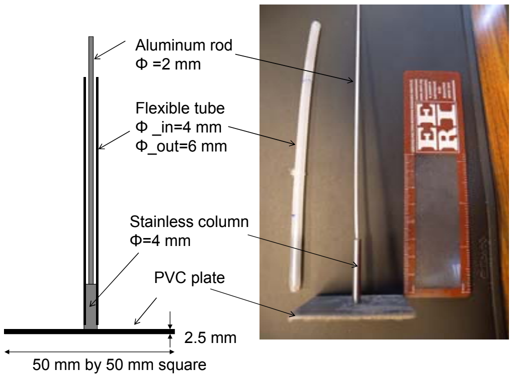

Figure 8 Detail of a settlement gauge

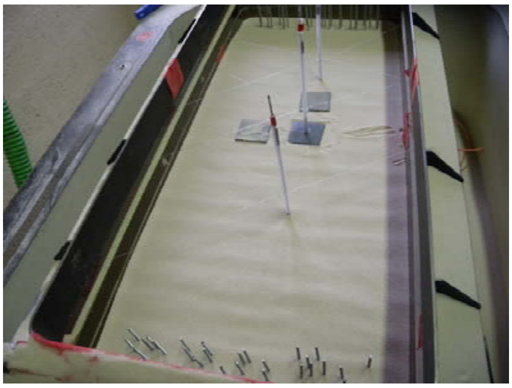

(a) Installation of settlement gauge

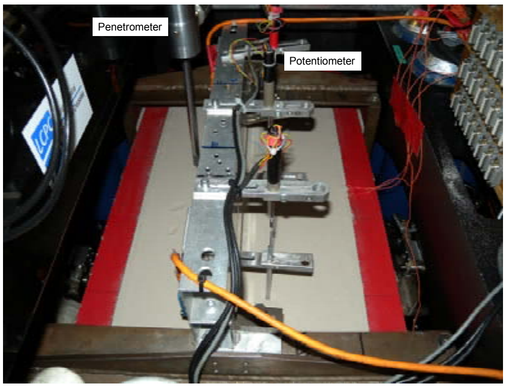

(b) Setup of penetrometer and potentiometers

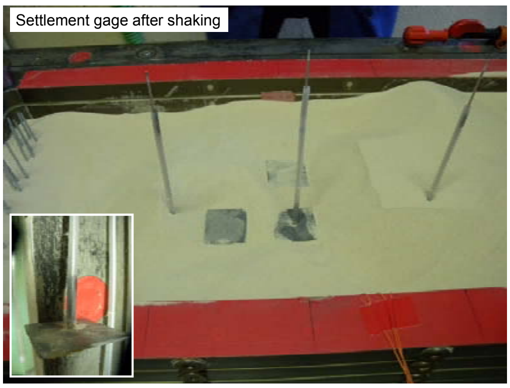

(c) Settlement gauges and PVC plates after the test

Figure 9 Model setup

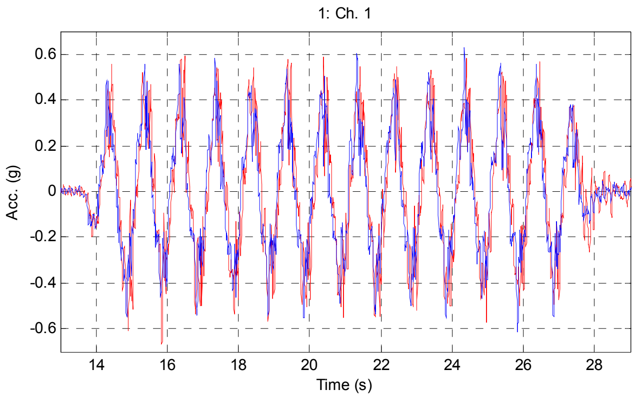

Figure 10 Time histories of input acceleration in prototype scale (red 25g_1, blue 50g_1)

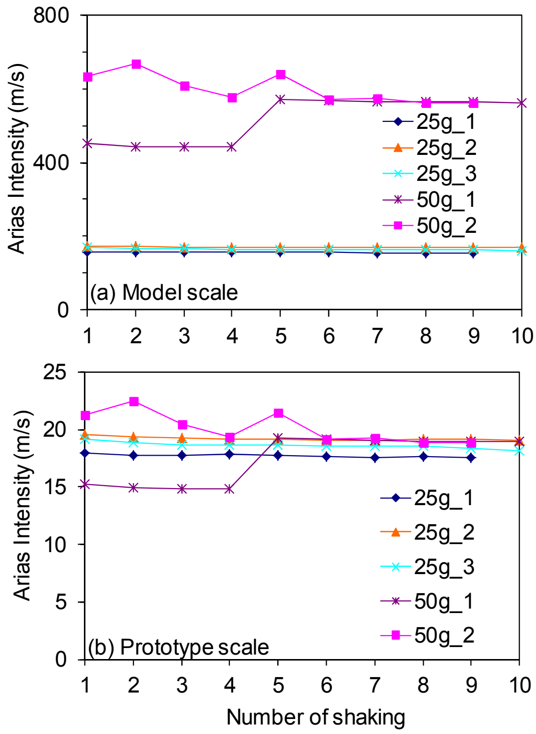

Figure 11 Arias intensity of the recorded input acceleration in prototype scale

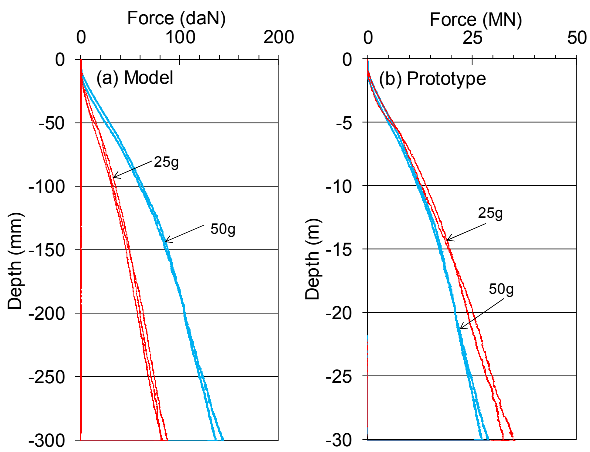

Figure 12 Penetrometer resistance before the initial shaking in model scale (a) and prototype scale (b)

The same trend can be observed in the profile after the 10th shaking (Figure 13). Degree of coincidence of the profile becomes lower especially in deeper depth. Small difference on shaking intensity in each shot can be accumulated to make such a large difference on the penetration resistance.

Although there are some variations, profiles of the resistance in prototype scale show more or less coincidence in prototype scale.

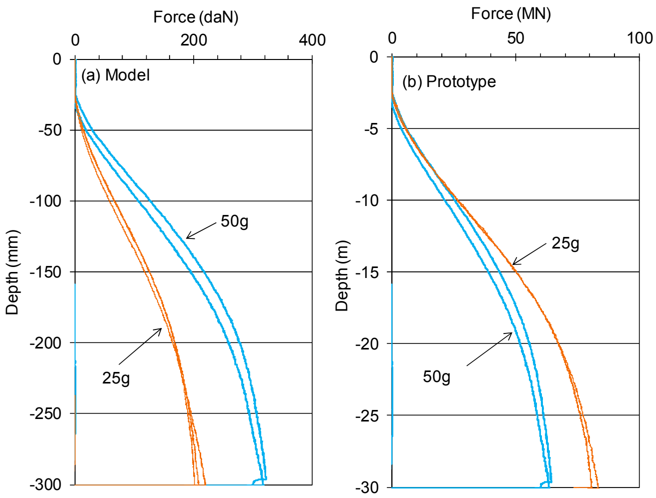

Figure 13 Penetrometer resistance after the 10th shaking in model scale (a) and prototype scale (b)

3.3 Ground settlements

Settlements at the ground surface are measured by laser displacement transducers, and those in the ground are by settlement gauges. Before shaking, the ground is consolidated by applying the specified centrifugal accelerations consecutively 3 times to stabilize the ground.

This process is manifested in Figure 14 (model scale). For example, as shown in Figure 14(a), as centrifugal acceleration increases, the ground surface settles about 1.1 mm (D122) to 1.3 mm (D116). After the centrifugal acceleration of 25 g being kept about 5 min (1st stabilization), centrifuge rotation is stopped (1 g). At this moment, the ground settlements are reduced to about 1 mm. Then again the centrifugal acceleration is applied, and as shown in Figure 14(a), the surface settlements further increases up to about 1.5 to 1.7 mm (2nd). This process is repeated 3 times. Common trend shown in Figure 14 is that the ground settles as centrifugal acceleration increases and in every application of centrifugal acceleration, the amount of ground settlements gradually increases. However, the rate of settlement is decreasing, i.e., the amount of settlement asymptotically approaches to some maximum values.

Figure 15 shows time histories of the ground settlements at all shaking steps. The curves indicate stepwise increase of settlements at each shaking. In Figure 15(b), the curve of D63 is increasing, i.e., settlement gauge is uplifted. This may be because of malfunctioning of the sensor or sands near the PVC plate were flowing under the plate.

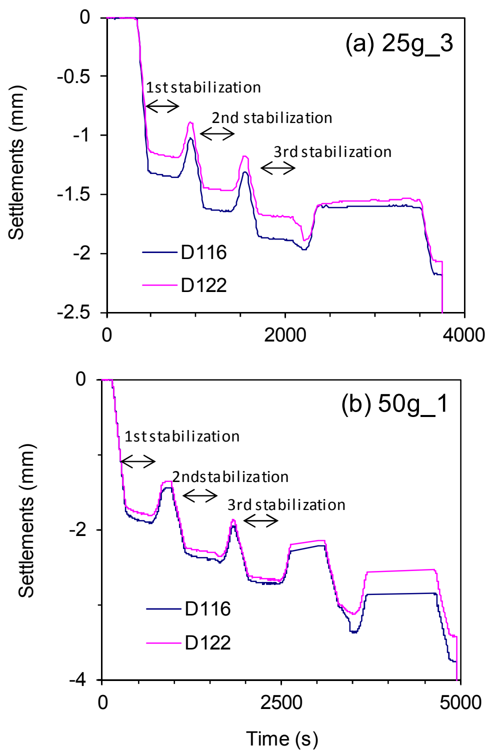

Figure 14 Time histories of ground settlements due to consolidation before shaking (model scale): (a) 25g_1 and (b) 50g_1

Amount of settlements at each shaking are summarized in Figure 16. If the generalized scaling law works correctly, settlements occurred at each shaking step should be identical. Results show [see Figure 16(a) for surface settlements], for example, that settlement after the 1st shaking is about 1,000 mm (2.4% of the total depth of 41.6 m) and values recorded by each sensor (D122 and D116) match well. However, as shaking continues, the difference of settlements measured under 25 g and 50 g seems to be increasing.

Since the amount of settlements after the initial shaking matched well compared with those in subsequent shaking, in what follows, settlements after the 1st shaking are investigated in terms of validation of the scaling law. Figure 17 compares settlements of all the sensors recorded after the 1st shaking for all cases. As mentioned earlier, case 50g_1 had lower and case 50g_2 had slightly larger intensity of shaking. This variation gives significant difference on the amount settlement as shown in Figure 17. Considering that the intensity of case 50g_2 is close to the ones in 25 g [Fig. 11(b)], the amount of settlement measured in the case of 50g_2 seems to be matching quite well with the cases of 25 g. The scaling factor of settlement (displacement) is as large as 200 for 25 g and 141 for 50 g, and considering possibility to have minor variation in constructing the model ground, in sensor setups, and in the input accelerations, these differences may be regarded as minor. Thus, the scaling law for settlement (displacement) may well be validated.

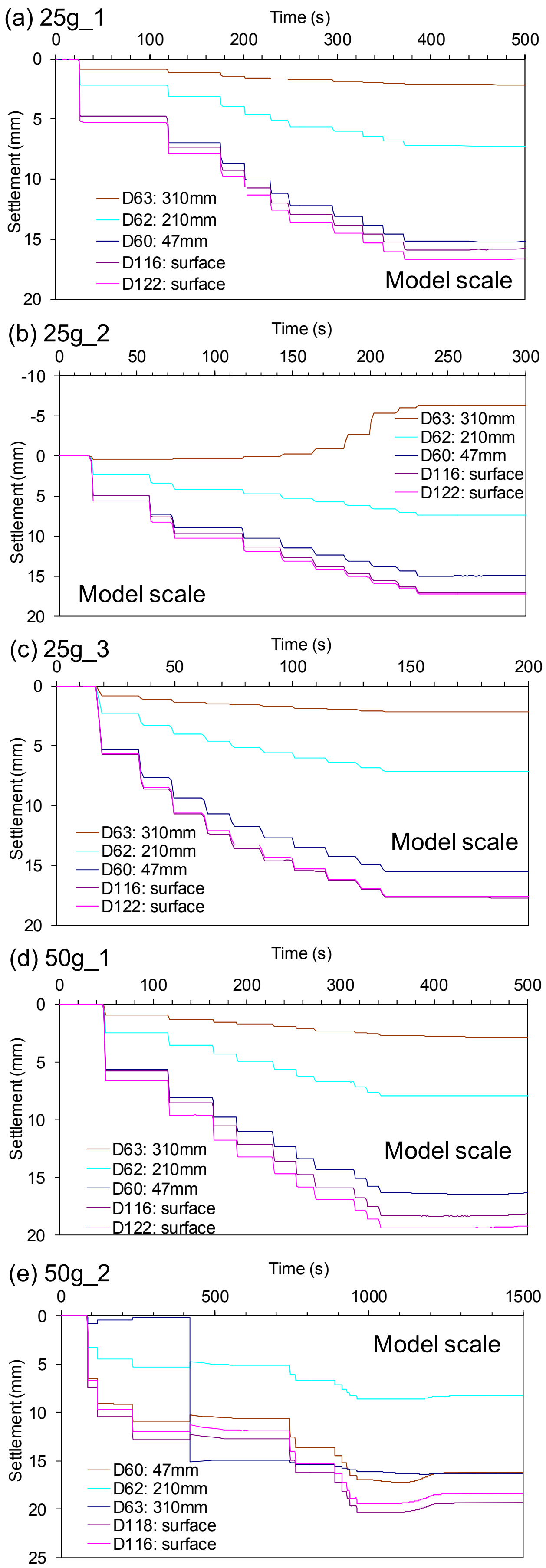

Figure 15 Time histories of ground settlements due to shaking (model scale)

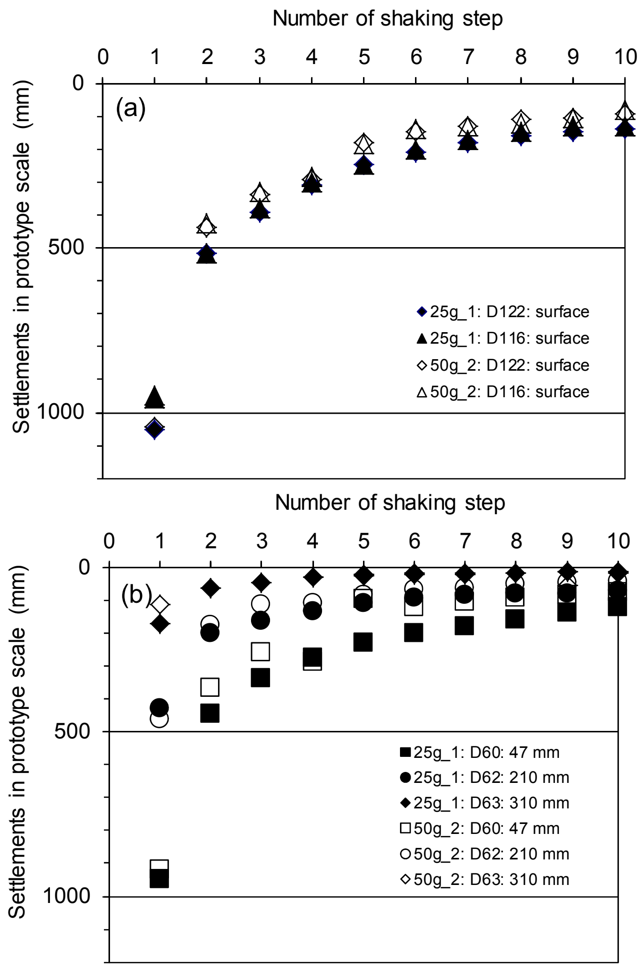

Figure 16 Settlements after each shaking in prototype scale: (a) surface, (b) in depth

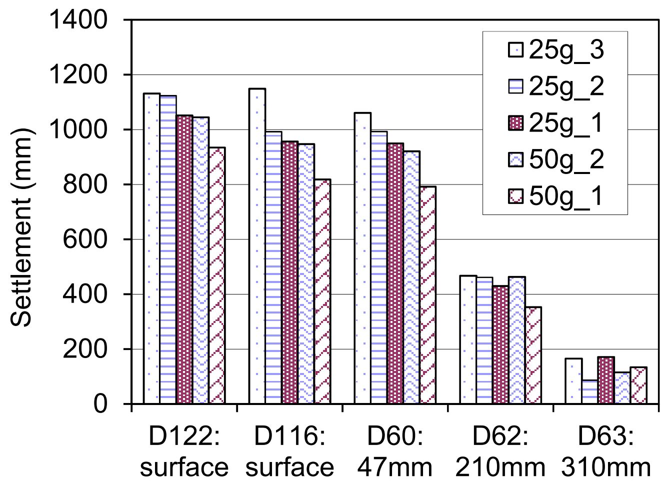

Figure 17 Summary of settlements measured after the 1st shaking in all the test cases in prototype scale

4. CONCLUSIONS

To examine the applicability of the generalized scaling law, a series of dynamic tests under two different centrifugal accelerations of 25 g and 50 g were conducted under the scheme of "modelling of models." In the ESB box, the model ground consisted of a flat dry sand layer with the relative density of 50% of the Fontainebleau sand NE34. A prototype ground and input accelerations were scaled down to 1/100 according with the scaling law. A sinusoidal input acceleration of frequency 1.0 Hz, maximum amplitude 0.5 g, and duration 14 sec in prototype scale was applied to the model ground. Each model was exposed to the identical input motion sequentially 10 times.

In terms of the Arias Intensity, the input accelerations given at the beginning of the cases of 50 g were slightly larger than that of the cases of 25 g. Although effect of this is manifested in the amount of settlements, measured settlements about 1 m (2.4% of the total depth of the model ground) after the initial shake in prototype scale showed significant agreements between the two models when the intensity of shaking was nearly identical. Thus, the applicability of the generalized scaling law for displacement is validated under 25 g and 50 g.

The soil resistance measured by the miniature penetrometer in prototype scale showed systematic variation between 25 g and 50 g, i.e., the soil resistance measured under 50 g is systematically smaller than the one obtained under 25 g. Cause of this is unknown yet, and further investigation is necessary to know the application limit of the generalized scaling law.

5. ACKNOWLEDGEMENTS

The authors would like to thank laboratory technicians at IFSTTAR, Nantes, France: Mr. Philippe Audrain, Mr. Claude Favraud, Mr. Patric Gaudicheau, Mr. Damien Macé, Mr. Alain Neel, and Dr. Gerard Rault, for their sincere assistance for conducting the centrifuge experiments reported in the present paper.

6. REFERENCES

Arias, A. (1970). A Measure of Earthquake Intensity. R.J. Hansen, ed. “Seismic Design for Nuclear Power Plants”. MIT Press, Cambridge, Massachusetts, pp438-483.

Einde, V. D., Restrepo, L., Conte, J. P., Luco, E., Seible, F., Filiatrault, A., Clark, A., Johnson, A., Gram, M., Kusner, D. & Thoen, B. (2004). “Development of the George E. Brown Jr. network for earthquake engineering simulation (NEES) large high performance outdoor shake table at the University of California, San Diego.” Proceedigns of the 13th World Conference on Earthquake Engineering, Vancouver, BC, Canada, 1-6 August, Paper No. 3281.

Garnier, J., Gaudin, C., Springman, S. M., Culligan, P. J., Goodings, D., Konig, D., Kutter, B., L., Phillips, R., Randolph, M. F. & Thorel, L. (2007). “Catalogue of scaling laws and similitude questions in geotechnical centrifuge modelling”. International Journal of Physical Modelling in Geotechnics 7, No. 3, pp1–23.

Haigh, S.K., Eadington, J., and Madabhushi, S.P.G. (2012). “Permeability and stiffness of sands at very low effective stresses”. Géotechnique, Vol. 62, No. 1, pp69–75.

Iai, S. (1989). “Similitude for shaking table tests on soil-structure-fluid model in 1g gravitational field”. Soils and Foundations, Vol. 29, No. 1, pp105–118.

Iai, S., Tobita, T. & Nakahara, T. (2005). “Generalized scaling relations for dynamic centrifuge tests”. Géotechnique, Vol. 55, No. 5, pp355–362.

Schofield, A. N. (1980). “Cambridge geotechnical centrifuge operations”. Géotechnique, Vol. 30, No. 3, pp227–268.

Tobita, T., Iai, S., von der Tann, L., and Yaoi, Y. (2011). “Application of the generalised scaling law to saturated ground”. International Journal of Physical Modelling in Geotechnics, Vol. 11, No. 4, pp138-155.

Tokimatsu, K., Suzuki, H., Tabata, K. & Sato, M. (2007). “Three dimensional shaking table tests on soil-pile-structure models using E-Defense facility”. 4th International Conference on Earthquake Engineering, June 25–28, Thessaloniki, Greece.